Technical and Economic Feasibility Assessment of Utilizing Renewable Energy Resources for Enhancing Energy Security and Freshwater Supply along the Makran Coast

Mohammad Javad Ghalandari[1,*], Mohsen Zali 2[2], and Kaveh Yazdi[1]

[1] *Faculty of Electrical Engineering, University of Noshahr, Noshahr, Iran.*
[2] *Faculty of the Mechanic, Malek Ashtar University of Technology, Tehran, Iran.*
**Corresponding author: jghalandari@ihu.ac.ir*

Manuscript received 21 June, 2024; revised 14 September, 2024; accepted 20 September, 2024. Paper no. JEMT-2406-1512.

The increase in population, natural disasters, the growth of energy-intensive industries and power plant aging are among the most significant threats to energy security in Iran. A geographic feasibility assessment, along with technical and economic optimization, was conducted in this study to supply electricity to a population of 50,000 residents on the Makran coasts. Simultaneously, the excess electricity has been used to meet the energy requirements of a seawater desalination plant in this high-water scarcity area. To determine suitable locations based on available infrastructure, the Geographic Information System (GIS) was employed. Ultimately, the methods for primary power supply were identified using a HOMER-MATLAB based multi-criteria decision-making approach. The results indicate that the certain parts of Jask, Konarak, Chabahar, and Beris regions, have the capability to host hybrid renewable plants. Additionally, with less than 19 MW of renewable power connected to the national grid, the reliability of the power supply has increased by over 99%. The final excess electricity has been reduced to less than 6%, annual CO_2 emissions have decreased by more than 30%, dependence on power transmission lines has decreased by over 40%, and energy costs are expected to decrease to less than $0.05/kWh.

Keywords: *Hybrid renewable optimization, Geographic Information System, Cost of energy, Energy security.*

http://dx.doi.org/10.22109/jemt.2024.464018.1512

1. Introduction

In Iran, most power plants are situated in the central regions of the country [1], contributing to a reduction in energy security in peripheral and coastal areas. The extensive transmission lines are highly susceptible to human and natural hazards, as well as wear and tear, resulting in higher maintenance costs. In some areas, transmission losses may exceed 12% [2]. Essential facilities such as hospitals and security centers rely on backup fossil fuel generators and battery banks during power outages. However, using this equipment for residential purposes is costly and requires widespread access to fuel. According to a NATO report [3] that emphasizes the importance of utilizing renewable resources, these sources contribute to localizing energy production, reducing the need for long-distance energy transmission lines, and diversifying energy supply sources, ultimately enhancing energy security. Iran faces the challenge of managing rapid consumption growth compared to the development of fossil fuel power plants and the aging of transmission lines. This challenge can lead to growing annual power outages, especially during peak periods (summer months) [4], and may limit the development of cities in tropical regions due to energy and water scarcity. Therefore, the economically viable use of renewable resources presents a strategic option to enhance energy security in the national power grid, particularly in developing regions and newly established cities. As of the end of July 2023, the installed capacity of renewable energy power plants in Iran amounts to 1050 megawatts. Among these, 360 MW are associated with wind power plants, more than 560 MW with solar power plants, and the remaining capacity is allocated to small hydropower plants (100 MW), biomass (15 MW), and other sources (10 MW) [5]. The three southern provinces of Iran, including the coasts of Makran in the vicinity of the Oman Sea, constitute less than 8% of the total renewable energy production, despite experiencing the high levels of energy and water tension in this region. Globally, the average capacity of power plants supplied by renewable energies is 30%. However, in Iran, the contribution of renewables is notably lower, constituting less than two percent of the

country's total power plant capacity [6].

Limited studies have been undertaken to assess the geographical potential of utilizing renewable resources on the southern coasts of Iran. Ghasemi et al. [7] conducted a study to evaluate the feasibility of constructing a solar power plant, considering natural, economic, and infrastructural constraints in Sistan and Baluchestan province. Despite being identified as capable of accommodating photovoltaic power plants over more than 50% of the province's area, only 14% is deemed ideal in terms of both infrastructure and natural conditions. Razeghi et al. [8], through GIS-based simulation, demonstrated that the coastal cities of Jask and Sirik have the potential to harness solar energy for power supply to reverse osmosis power plants. Hooshangi et al. [9] showed that, among the coastal cities near the Oman Sea in Iran, Jask and Chabahar regions have a greater potential for affordable power supply plants. Although most areas in Iran benefit from desirable solar radiation due to their proximity to the equator, specialized GIS analysis is required to accurately assess wind speed. Asadi et al. [10], through countrywide GIS analysis, determined that approximately 2% of the country's total area possesses favorable potential for harnessing wind power. Among these areas, Sistan and Baluchestan, as well as Khorasan provinces, were identified as having the highest number of optimal sites for establishing wind turbine power plants. Their mapping also evaluated some locations along the southern coasts of the country, recognizing the need for specialized regional assessments to precisely identify these areas. Dehkordi et al. [11] suggested that for regions where wind speed potential is not suitable throughout the year, a combination of wind, solar, and even local biomass energy can lead to more consistent energy production, overcoming energy challenges. Eastern sections of the southern coasts of Iran, such as Bandar Abbas, Jask, and Sirik, cannot rely on wind as a permanent and reliable source to meet the needs of coastal residents. Therefore, the integration of renewable resources in these areas can provide a more reliable and accessible supply of renewable energy.

The main renewable resources in the southern coast of Iran are not limited to solar and wind potentials. Studies on harnessing energy from sea waves in Iran have primarily focused on estimating available wave power, with limited emphasis on the technical and economic performance assessments of wave energy converter (WEC) devices. This lack of emphasis is attributed to the underdeveloped nature of WEC technologies for constructing such devices in Western Asia [12]. Jahangir et al. [13] estimated the average power potential extractable from each square meter of the Caspian Sea to be between 1.5 and 3 kWh/m^2. Kamranzad et al. [14] calculated this value for the Persian Gulf to be between 1 and 3 kWh/m^2. Finally, Rashid et al. [15] estimated this value to be over 2 kWh/m^2 on the coasts of Iran adjacent to the Oman Sea. Considering that global commercial devices are generally developed for waters with an average exceeding 6 kWh/m (commonly observed in oceans) [16], it can be inferred that WEC technologies may not be highly efficient on the southern coasts of Iran. Nasrollahi et al. [17] conducted an analysis of 28 commercially available WECs with the aim of identifying the most optimal device based on indicators of sustainable development for Iran. The criteria for selecting the superior device were grounded in strategic, technical, technological, economic, and environmental factors. Their multi-criteria decision-making process showed that the Pelamis device is a promising option for harnessing energy from local waves. Among other devices, Wave Roller, Anaconda Converter, AquaBuOY, and Oyster were also considered as potential optimal solutions, although comprehensive technical and economic analyses for these devices are yet to be conducted.

As can be seen, the majority of previous studies have focused on simple geographical feasibility studies of renewable plants, neglecting the techno-economic justifications for the southern coast of Iran. This is particularly notable in the case of the Makran region, which has not received specialized attention in previous studies due to the newly codified plan for the development of this area. But the effective application of hybrid renewable energy systems (HRESs) in other regions of Iran has been proved by international studies. Asrari et al. [18] conducted a study on the economic and environmental benefits of hybridizing solar and wind resources in conjunction with the national electricity grid in the city of Mashhad. They demonstrated that, in the long term, the high initial investment cost could be offset by the reduced cost of energy and decreased CO2 emissions from the hybrid system. Furthermore, Ref. [19] showed that, considering subsidized electricity tariffs in Iran, the affordability of stand-alone renewable systems can be much lower compared to grid-connected hybrid systems. Jahangiri et al. [20] investigated the utilization of grid-connected systems, comprising solar panels and battery banks, for residential applications in all climatic regions of the country, excluding grid subsidies. The results indicated that, despite the warm and tropical climates of the southern coastal cities of Iran, these areas possess the highest economic potential. This is attributed to their high solar radiation potential, resulting in energy costs of less than 0.161 $/kWh. Additionally, Kasaeian et al. [21], through a comprehensive sensitivity analysis, calculated the energy costs of grid-connected renewable energy systems in Iran to range between $0.09 and $0.235 per kWh. This calculation was based on potential variations in economic conditions and renewable potential. In coastal areas of the southern part of the country, Jahangiri et al. [22] demonstrated that hybrid grid-connected systems, incorporating solar panels and wave energy conversion systems, can provide energy to the coastal line of the Persian Gulf with maximum reliability and energy costs of less than 0.15 $/kWh.

The higher contribution of renewable energy in the power supply process can lead to increased energy security by minimizing grid dependency and localizing power generation. However, due to the intermittent nature of renewable energies, this may result in a surplus of power [23]. Excess electricity can be injected into the grid for consumption in other applications [24]. In mini-microgrids, it can improve self-utilization of power and minimize potential losses. Vaziri Rad et al. [25], in their review of prevalent methods to manage the challenge of excess electricity in highly renewable energy systems, concluded that applying secondary loads with deferrable nature, such as water desalination units, irrigation systems, and electrolyzers, is highly effective. This approach not only reduces excess electricity levels but also derives additional benefits from the renewable power surplus. In coastal areas, desalination units based on electrical energy, such as reverse osmosis plants, can be prioritized for this purpose. Islam et al. [26] demonstrated that, by applying reverse osmosis plant along with renewable systems, the maximum surplus power will be close to 7% of the served demand. Additionally, references [27] and [28] indicated a range of 3.8% to 9.3% excess electricity levels and energy costs ranging from $0.105 to $0.238 per kWh in optimum scenarios using this approach.

According to the literature, countercurrent analysis of the optimum geographical location for implementing hybrid systems and techno-economic assessments of potential HRESs are not considered in the national development program. Furthermore, previous studies have not utilized surplus renewable power to address water scarcity while meeting large-scale residential demands. Due to the Iranian government's program for the development of residential areas and new cities in the southern coastal regions, this study analyzes the potential of applying a hybrid system comprising photovoltaic panels, wind turbines, and wave energy converters to enhance grid reliability in the Makran region. To this end, the study first identifies potential near coast locations for solar and wind power plants using geographical information system (GIS) tools. Subsequently, the average available renewable resources in these areas are input into the HOMER software for the techno-economic analysis of HRESs. The

optimal power supply solutions are then prioritized using Multiple-Criteria Decision-Making (MCDM) methods implemented in MATLAB software. Finally, a sensitivity analysis has been conducted on the optimum scenario to assess the resilience of the power supply solution.

2. Methodology

In Sections 2.1 to 2.4, the optimization process, load and resource data, method and inputs for GIS assessment, as well as the formulation of decision-making objectives, the AHP method, and the TOPSIS process, are presented respectively. The data related to prevalent residential power consumption components and their rated capacities were obtained through field research. The 15-year average data (2005 to 2020) on solar and wind potential were downloaded from NASA's meteorological database and cross-checked with 2022 data from the Iranian Meteorological Organization. For the economic input data, the names and prices of common equipment in Iran were first estimated from companies active in this field. Then, scientific articles related to energy system construction in Iran, with prices closest to the estimated values, were selected as references.

2.1. Hybrid System Modeling

Figure 1 illustrates the working principle of the optimization process in this study. Initially, optimal site locations in the Makran area were identified through GIS assessment, considering topological, environmental, technical, and constraint data layers. If the consistency ratio of the weighted layers determined by the AHP method was less than 0.1, the average wind speed and solar radiation of the ideal sites were input into the HOMER software. The HOMER optimizer determined the best combination of renewables to address potential blackouts, thereby enhancing power supply reliability and energy security. In each time step (on an hourly basis), the output power of selected sizes of renewable components was determined based on the available potential of renewable resources. If the generated power by the renewable component (P_{Ren}) exceeds the remaining load (P_{Load}), the load is supplied, and the state of charge (SOC) of the battery bank and the storage tank level (DF) for the deferrable load (desalination unit) are determined. Available excess electricity from renewable resources is sent to the battery bank and then used to enable the desalination plant pumps, thereby improving the self-consumption of the generated energy. If there is still surplus power, it will be either injected into the local grid for use in other possible applications or dumped.

On the other hand, if the generated power by the renewables is less than the remaining demand to be supplied by non-grid resources, the battery bank State of Charge (SOC) is checked. When the battery bank is empty, the system considers a loss of power supply (LPSP) up to the allowable level in each time step. In this study, the maximum capacity shortage is considered to be 2% for residential applications. If the renewable power can meet the remaining load subtracted from the capacity shortage (P_{LPSP}), then the load is supplied, and the cumulative LPSP from previous time steps is calculated. In cases where cumulative LPSP exceeds the maximum allowable LPSP, or when the renewables still cannot supply the remaining load, the scenario is considered unfeasible. If there is any charge content in the battery bank, it is first discharged, and then the mentioned process is repeated. The renewable configurations that can supply power for all 8760 hours of the year are considered feasible scenarios, and output objectives such as the Cost of Energy (COE) and Renewable Fraction (RF) are calculated for them. Finally, the determined values are imported into the MATLAB-based MCDM process to classify the optimal scenarios based on the TOPSIS optimality factor for the Makran region.

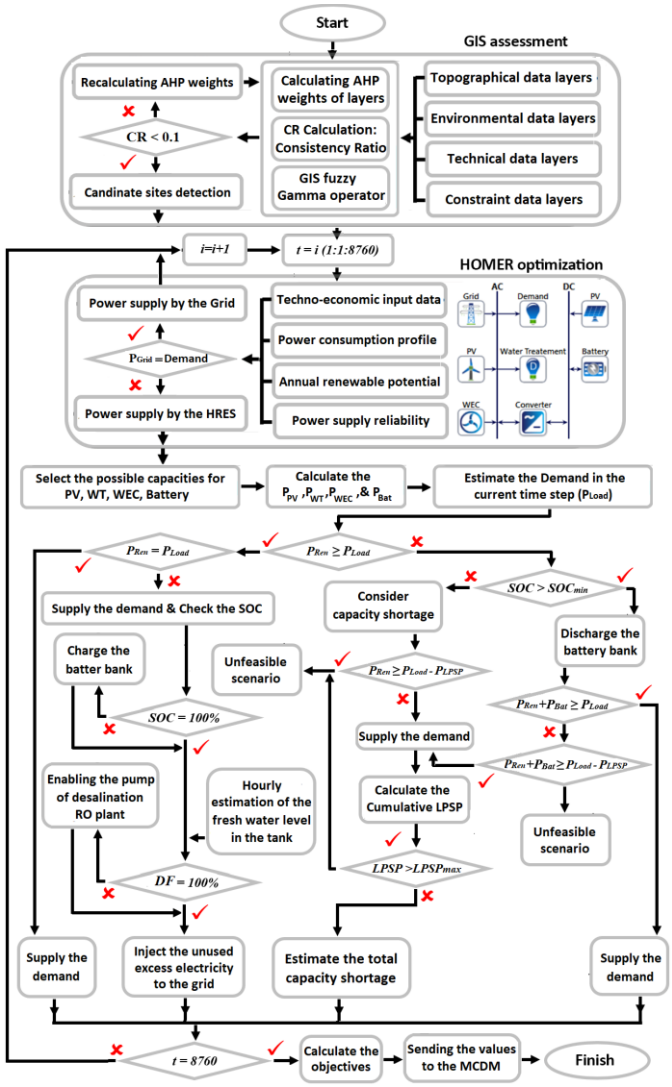

Fig. 1. The brief working principle of the hybrid system dispatch strategy during the optimization process

2.2. Electrical Load and Renewable Resources

Table 1 illustrates the maximum average daily power consumption of a household in the Makran region. Accordingly, each household consumes a maximum of 20 kWh/day of electrical power. The objective of this study is to supply a medium-sized city with 50,000 residents, equivalent to approximately 10,000 households. Therefore, the maximum electrical demand will be approximately 200 MWh/day. To calculate the monthly load peak, the HOMER load estimator is utilized. The software takes into account the warm and humid climate conditions, the residential consumer type, maximum consumption of each unit, the number of units, and geographical coordinates. Additionally, a maximum daily error of 2% and a maximum hourly error of 2% in the estimated values have been assumed to enhance the flexibility of the simulation results, considering possible changes in the primary load. The estimate monthly peak with the maximum value (26.7 MW) at July can be observed in Fig. 2.

In warm climates, the maximum daily fresh water requirement per resident is reported to be approximately 0.03 m^3/day, as indicated in Ref. [29]. According to Refs. [30], [31], and [32] a reverse osmosis (RO) plant typically requires an average energy consumption of 2.5-4 kWh/m^3 to desalinate seawater. For the purposes of this study, the upper value of 4 kWh/m^3 is chosen. Due to uncertainties in the location of the desalination plant, the energy required for pumping seawater to

the plant pond is disregarded. Consequently, to meet the fresh water needs of 50,000 residents through the RO plant, a total energy consumption of 6000 kWh/day is estimated. The peak power demand, equivalent to the power consumption of the water transfer pump from the pond to the device (25%), the pump facilitating water passage through the membrane (60%), and the pump for transferring water to storage reservoirs (15%), is calculated to be up to 300 kW.

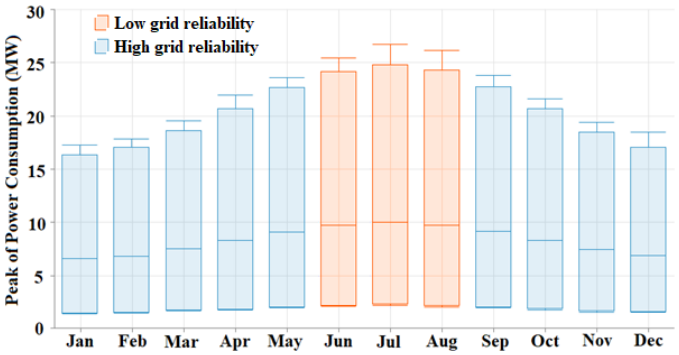

Fig. 2. Monthly power consumption for targeted households

Table 1. Maximum power consumption for a typical residential unit in the Makran region (based on field research)

Device	Operation (Hours)	Quantity (Units)	Rated Power (W)	Energy Consumption (kWh/d)
Food Refrigerator	24	1	200	4.8
TV set	12	1	100	1.2
Indoor Lighting	12	5	20	1.2
Air Conditioner	10	1	400	4.0
Mini Fan	12	1	60	0.7
Electrical Heater	3	1	1200	3.6
Charger	1.5	2	100	0.3
Other	1	1	2000	2
Average energy demand per household				20.0

Figures 3 to 5 depict the climatic and renewable resources potential in the study area. Solar radiation consistently exceeds 4 kWh/m^2 throughout the year, peaking at over 7 kWh/m^2 during the summer months. Additionally, the average sky clearness index surpasses 60%, creating an ideal condition for harnessing solar energy. The average wind speed varies between 3.5 and 6.1 m/s, emphasizing the need for a thorough site location analysis for the establishment of wind turbine plants. Moreover, the frequency of dusty days increases during the summer months, posing a challenge for the operation and maintenance of renewable systems. In contrast, during other seasons, it remains within an acceptable range, with fewer than 5 days. The 24-hour average ambient temperature ranges from 31-35°C in the summer and 19-21°C in the winter, indicating the warm climate of the Makran area. This underscores the importance of considering the negative effects of high temperatures on PV power output. Furthermore, the ambient air humidity remains within the range of 60-80% throughout the year.

Finally, Fig. 6 illustrates the significant wave height in regions within 50 km of the coastlines of Makran in the Oman Sea. Throughout most periods of the year, the average wave height remains consistently below 2 m, with minimum values occurring during the summer season. Furthermore, according to information provided by the Ports & Maritime Organization of Iran [33], these areas experience a wave period of less than 6 seconds, which improves in higher distances from the coastline and in areas closer to the Indian Ocean.

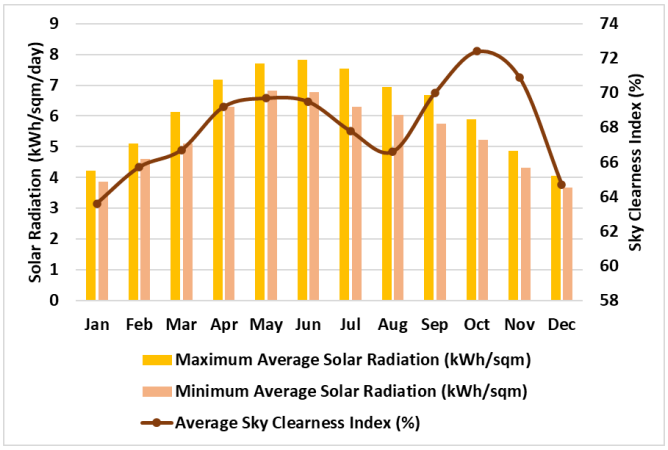

Fig. 3. Monthly averages of solar radiation and sky clearness index in Makran region [34]

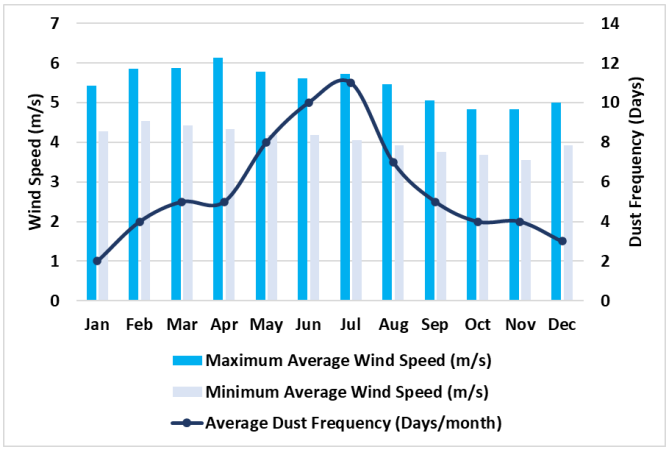

Fig. 4. Monthly averages of wind speed and dusty days frequency in Makran region [34]

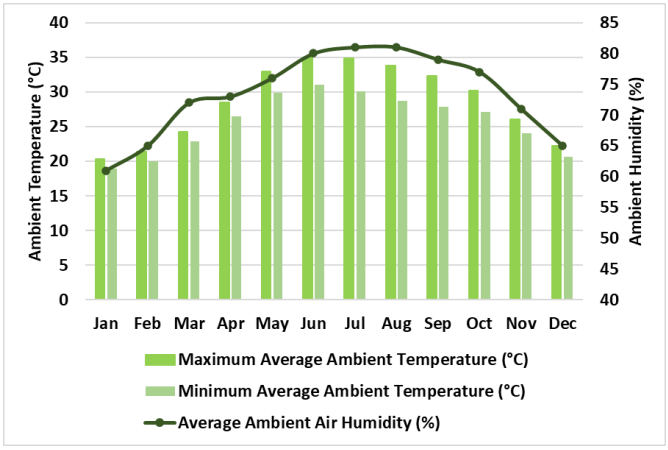

Fig. 5. Monthly averages of ambient temperature and air humidity in Makran region [34]

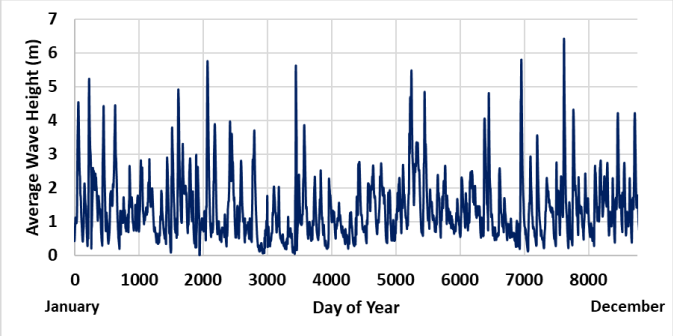

Fig. 6. Annual significant wave height in the Oman Sea in areas within 50 km of the coastline [33]

2.3. Geographical Information System Assessment

The Analytic Hierarchy Process (AHP), devised by Thomas L. Saati [35], is a applied to weight the applied layers in the GIS software. It involves breaking down a problem into main goals, criteria, sub-criteria, and alternatives to ascertain the relative significance of each for achieving the primary objective. In this study the methodology of this process including the fundamental scale and random index selection and also the applied formulation (as follows) applied based on the study of Dehghan et al. [36]:

$$A = \begin{bmatrix} 1 & a_{12} & \cdots & a_{1n} \\ a_{21} & 1 & \cdots & a_{2n} \\ \vdots & \ldots & \ddots & \vdots \\ a_{n1} & a_{n2} & \cdots & 1 \end{bmatrix} \quad (1)$$

$$a_{ji} = \frac{1}{a_{ij}} \quad (2)$$

$$det(A - I\lambda) = 0 \quad (3)$$

$$(A - I\lambda_{max}) \times W = 0 \quad (4)$$

$$CI = \frac{\lambda_{max} - n}{n - 1} \quad (5)$$

$$CR = \frac{CI}{RI} \quad (6)$$

$$LDI_i = \left(\sum_{j=1}^{7} W_j \, x_{ij}\right) . \prod_{k}^{4} EC_{ik} \quad (7)$$

$$\text{Optimality} = \begin{cases} LDI = 0 \rightarrow Constraint\ area \\ 1 \le LDI < 3 \rightarrow Not\ desirable \\ 3 \le LDI < 5 \rightarrow Less\ desirable \\ 5 \le LDI < 7 \rightarrow Desirable \\ 7 \le LDI \le 9 \rightarrow Most\ desirable \end{cases} \quad (8)$$

In the first step, a decision-making hierarchy tree must be created with the main goal at the top (wind and solar site selection) and the necessary criteria, including environmental, technical, and topographical, which must be derived from the constraint map. Criteria can be further divided into sub-criteria, as shown in Table 2. In the second step, the importance of sub-criteria has been evaluated using a pairwise comparison. Experts use a nine-point scale based on the fundamental scale of Saaty to prioritize the importance of layers. Equation (1) illustrates a sample matrix for pairwise comparison, where 'n' is the number of criteria, and 'a_{ij}' represents the relative importance of criteria compared to 'j'. In the third step, Equation (3) is applied to set the determinant of the matrix (A-Iλ) to zero and calculate λ. Subsequently, the highest λ (λ_{max}) is placed into Equation (4) to obtain the weight of each sub-criterion. In the fourth step, the Consistency Index (CI) has been computed based on λmax and the number of sub-criteria (Equation (5)). Then, the consistency ratio (Equation (6)) has been determined using CI and the Random Index (RI). It should be noted that the random index has been selected based on Saaty's table corresponding to the number of weighted criteria, approximately 1.11 in this case. If CR < 0.1, the matrix is consistent, and the weights are reasonable for entry into GIS software. If CR > 0.1, a pairwise comparison must be repeated until CR is below 0.1. In the last step, the final value of each pixel (0.3 km × 0.3 km) on the map has been calculated using equations (7) and (8). Where LDI is the land desirability index, W_j is the assigned weight to criteria j, and x_{ij} is the standard value of i under the reclassification of criteria j. Furthermore, EC_{ik} assigns an optimality weight of zero to areas with constraints for developing renewable power plants, ensuring they are not considered in the optimization process. Finally, a CI of less than 0.05 and a CR of less than 0.1 have been achieved with the weights provided in Table 2. These weights are then imported into GIS software for optimal site selection.

Table 2. Criteria and sub-criteria of weighted and constraint layers applied in the GIS assessment

Criteria	Sub-criteria	AHP weight
Climatic	Average wind speed [37]	55%
	Average solar radiation [9]	
Technical	High load demand areas and their transmission lines [38]	12%
	Main transportation roads [39]	15%
	Areas with legal prohibitions (non-issuance of permits for installation)	0
Environmental	Protected areas	0
	Main permanent rivers [39]	8%
Topological	Faults and Elevations [40]	0
	Ground surface slop [41]	10%

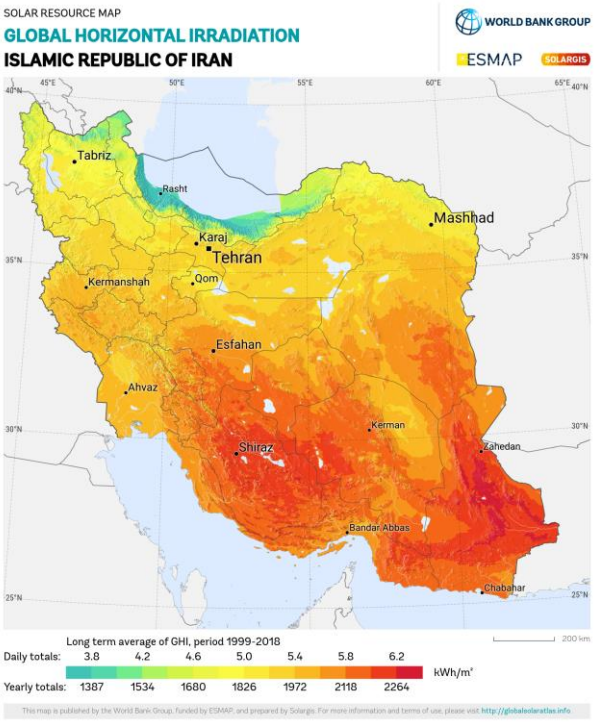

Fig. 7. Solar radiation map of the Iran (applied in the GIS assessment) [42]

In Table 2, criteria with a zero value represent constraint layers that exclude certain areas from potential renewable installation sites. Additionally, other weighted areas contribute to the estimation of the land desirability index, indicating the overall suitability of each area in the Makran region. Wind and solar site selection has been conducted separately to account for the possibility of incorporating a battery bank, allowing for the operation of a hybrid power plant. Table 3 presents the categorical classification of geographic layers used in the GIS process.

Table 3. Classification of geographic layers based on range of desirability

Value	Wind Speed	Solar Radiation	Distance from the Rivers	Distance from the Roads	Ground Surface Slope	Distance from the load centers
Unit	m/s	W/m2	km	km	%	km
0	< 7	< 3.5	0-1	0-0.5	> 10	0-2
1	7-9	3.5-4	> 16	16-20	9-10	> 45
2	9-11	4-4.5	14-16	14-16	8-9	40-45
3	11-13	4.5-5	12-14	12-14	7-8	35-40
4	13-15	5-5.5	10-12	10-12	6-7	30-35
5	15-17	5.5-6	8-10	8-10	5-6	25-30
6	17-19	6-6.5	6-8	6-8	4-5	20-25
7	19-21	6.5-7	4-6	4-6	3-4	15-20
8	21-23	7-7.5	2-4	2-4	2-3	10-15
9	> 23	> 7.5	1-2	0.5-2	< 2	2-10

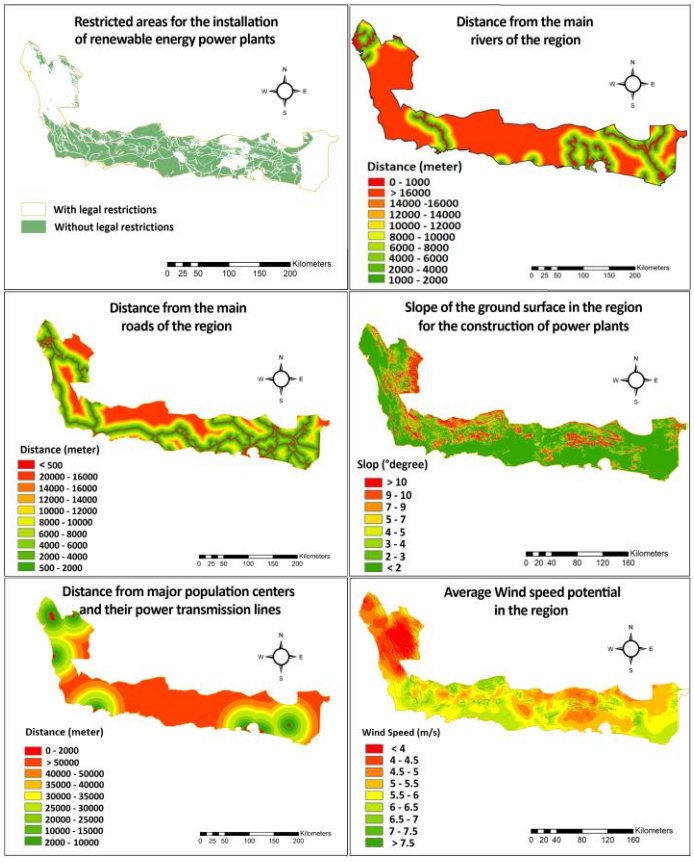

Fig. 8. Applied reclassified maps of the Makran region in the GIS assessment

Figure 7 shows the solar radiation atlas of Iran. As can be seen, all of the Makran region along the southern coasts has solar radiation higher than 5.6 kWh/m². Therefore, all of the regions are desirable for solar availability. However, according to Fig. 8, other layers demonstrate significant changes in optimality in different locations of the Makran region. Therefore, the GIS assessment classifies the regions based on their optimality in achieving a higher desirability factor according to the weights and restrictions.

2.4. Main Equations

In this section, the main power output equations applied in the HOMER software [43] and the MCDM process in MATLAB software [44] are described. The PV power output calculate based on Eqs. 9 to 11. where f_{PV} is the percentage of derating factor, Y_{PV} is the rated kW of installed modules, G_{Total}, and $G_{T.STC}$ are the the total kW/m^2 solar radiation on the PV surface at real and standard conditions, respectively. Also, μ presents the negative effect of temperature on output power (0.4 %/°C [45]), and T_c is the PV cell temperature. Accordingly, $T_{c,NOCT}$ and $T_{a,NOCT}$ are the temperature of cell and ambient at NOCT, respectively. $\eta_{mp,STC}$ shows the maximum power point efficiency (%), α is the percentage of radiation absorptance by the module, and τ is the percentage of solar transmittance in the PV glass cover.

$$P_{PV} = Y_{PV} f_{PV} \left(\frac{G_T}{G_{T.STC}}\right)[1 + \mu\,(T_c - T_{c.STC})] \tag{9}$$

$$\eta_{PV} = \eta_{PV,STC}\left(1 + \frac{\mu}{\eta_{PV}}(T_a - T_{STC}) + \frac{\mu}{\eta_{PV,STC}}\frac{a + bV_{NOCT}}{a + bV}\frac{NOCT - 20}{800}(1 - \eta_{PV,STC})G_T\right)\Psi \tag{10}$$

$$T_c = \left(\frac{T_a + (T_{c,NOCT} - T_{a,NOCT})\left(\frac{G_T}{G_{T.STC}}\right)\left(\frac{[1 - \eta_{mp,STC}(1 - \mu.T_{c.STC})]}{\alpha\tau}\right)}{1 + (T_{c,NOCT} - T_{a,NOCT})\left(\frac{G_T}{G_{T.STC}}\right)\left(\frac{\mu.\eta_{mp,STC}}{\alpha\tau}\right)}\right) \tag{11}$$

The wind turbine power output can be calculated by Eq. 12 to Eq. 16. Where P_{WT} is the real output power of wind turbine and $P_{WT,STP}$ denotes it at the standard test condition. This parameter can changes based on the density of air (kg/m^3) and wind speed (m/s) at different heights (between anemometer and hub height). Furthermore, Eq. 12 shows applicable power generator from each wind turbine based on its rated power (P_{rated}), cut in and cut off wind speeds (V), and power curve constants (a and b). The power curve for the Vestas V47, one of the largest prevalent wind turbines in Iran, is depicted in Fig. 9 (a).

$$P_{WT} = \left(\frac{\rho}{\rho_0}\right)P_{WT,STP} \tag{12}$$

$$U_{hub} = U_{anem}\frac{ln(Z_{hub}/Z_0)}{ln(Z_{snem}/Z_0)} \tag{13}$$

$$P_{WT,STP} = \begin{cases} 0 & V \le V_{cutin} \\ a.V^3 - b.P_{rated} & V_{cutin} \le V \le V_{rated} \\ P_{rated} & V_{rated} \le V \le V_{cutoff} \\ 0 & V > V_{cutoff} \end{cases} \tag{14}$$

$$a = \frac{P_{rated}}{V^3{}_{rated} - V^3{}_{cutin}} \tag{15}$$

$$b = \frac{V^3{}_{cutin}}{V^3{}_{rated} - V^3{}_{cutin}} \tag{16}$$

Equation 17 represents the maximum theoretical output power achievable from wave energy converters (WECs) [12]. where, ρ denotes the density of water, T is the wave period in seconds, H represents the wave height, and L_{max} is the maximum body length of the wave energy converter (WEC) influenced by significant waves. It's important to highlight that the actual output power of each WEC can be determined using the device power matrix provided by the manufacturer. The power matrix for the PELAMIS wave energy converter, recognized as a potential and commercially available WEC, is illustrated in Fig. 9 (b).

$$P_{WEC.max} = \frac{\rho g^2 T H^2}{64\pi}.L_{max} \quad (17)$$

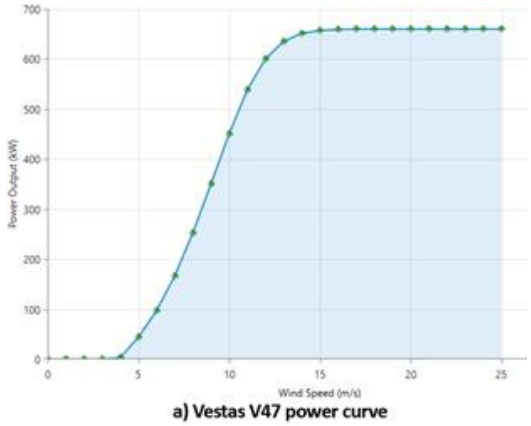

a) Vestas V47 power curve

Pelamis 750 kW	Wave Period (second)								
Wave Height (meter)	5	5.5	6	6.5	7	7.5	8	8.5	9
1	0	22	29	34	37	38	38	37	35
1.5	32	50	65	76	83	86	86	83	78
2	57	88	115	136	148	153	152	147	138
2.5	89	138	180	212	231	238	238	230	216
3	129	198	260	305	332	340	332	315	292
3.5	0	270	354	415	438	440	424	404	377
4	0	0	462	502	540	546	530	499	475
4.5	0	0	544	635	642	648	628	590	562
5	0	0	0	739	726	731	707	687	670

b) PELAMIS 750 power matrix

Fig. 9. Power generation potential compared to the available resources: a) Power curve of wind turbine and b) Power matrix of wave energy converter

$$RF = 1 - \frac{p_{Nonrenewable}}{p_{Useful}} \quad (18)$$

$$CO_2 = \Sigma P_{Grid}, E_{NG} \quad (19)$$

$$UL = \frac{P_{Unmet}}{p_{Load}} \quad (20)$$

$$SD = \frac{NOR_{Utilized}}{NOR_{Total}} \quad (21)$$

$$EX = \frac{p_{Excess}}{p_{Usefull} + p_{Excess}} \quad (22)$$

$$COE = \frac{C_{annual,total}}{P_{Usefull}} \quad (23)$$

$$C_{annual,total} = CRF(i.L_{Project}), C_{NPC,total} \quad (24)$$

$$CRF(i,L) = \frac{i(1+i)^L}{(1+i)^L - 1} \quad (25)$$

$$i = \frac{i^{\circ} - f}{1+f} \quad (26)$$

$$IC = \Sigma C_{Component}, N_{Component} \quad (27)$$

Equations 18 to 27 outline the computation of decision-making objectives (based on [46] and [47]). The renewable fraction can be determined using Equation 18. Additionally, the annual CO_2 emissions resulting from purchased power from the grid (P_{Grid}) and the emission factor (E_{NG}) of natural gas-based plants in Iran (660 g/kWh [48]) are calculated using Equation 19. The unmet load, or the ratio of capacity shortage (P_{Unmet}) to the primary load, is determined by Equation 20. Supplier diversity is calculated based on the number of individual power sources ($NOR_{Utilized}$) relative to the total available sources in the area (NOR_{Total}). The excess electricity level (EX) can be calculated as the ratio of unused power (P_{Excess}) to the total generated power. The cost of energy (COE) is determined by Equations 23 to 26, considering the inflation rate (i), discount rate (f), net present cost (NPC), and project lifetime (L). Finally, Equation 27 is applied to ascertain the initial cost of HRES based on the number and capacity of applied power components [49]. Table A1 in Appendix A indicates all techno-economic input data of the HRESs.

As can be seen, the decision-making objectives can exhibit different optimality in each feasible power supply scenario. Therefore, the multicriteria decision-making process can help reach an optimal solution from all criteria's points of view. The initial decision matrix (X) encompasses objectives, options, and a weight matrix (W) within the multi-criteria decision-making (MCDM) framework. The weights of objectives in this study have been determined by the AHP-based subjective process involving the policy makers. The resulting weights were about 19%, 18%, 14%, 8%, 16%, 14%, and 11% for the COE, IC, RF, CO_2, EX, UL, and SD decision-making criteria. A specific set of parameters, outlined in Eq. 28, needs to be defined to initiate the MCDM process using The Technique for Order of Preference by Similarity to Ideal Solution (TOPSIS) method. Subsequently, the normal matrix is defined as Eq. 29, and the k value is determined (Eq. 30) based on the number of involved parameters (m) in the decision-making process. Following this, Eqs. 31 and 32 are employed to determine the estimated entropy value for each criterion, forming the final weight matrix. According to Eqs. 33 and 34, a normalized decision matrix is then formed, and the weights are multiplied in this matrix. In the next step, the positive ideal solution and the negative ideal solution need to be calculated based on Eq. 35. Subsequently, the distance of each solution from the optimal solutions must be calculated using Eqs. 37 and 38. Finally, the numerical value of the performance factor (indicating the degree of proximity of results to the optimal solution) is calculated. A higher numerical value for the performance factor (C_j) of a scenario signifies a higher efficiency for that scenario [50].

$$X = \{x_{ij}\} \quad and \quad W = [w_i] \quad (28)$$

$$N_{ij} = \frac{x_{ij}}{\sum_{i=1}^{m} x_{ij}} \quad (29)$$

$$k = \frac{1}{\ln m} \quad (30)$$

$$E_j = -k \sum_{i=1}^{m} N_{ij} \,.\, ln\, N_{ij} \quad (31)$$

$$w_j = \frac{(1-e_j)}{\sum_{j=1}^{n}(1-e_j)} \quad (32)$$

$$R = \frac{x_{ij}}{\left(\sum_{i=1}^{m} x_{ij}^2\right)^{0.5}} \quad (33)$$

$$V = R \times W \quad (34)$$

$$A^+ = (v_1^+, \dots, v_m^+) \;\&\; A^- = (v_1^-, \dots, v_m^-) \quad (35)$$

$$S^+ = \sqrt{\sum_{i=1}^{m}\left(v^+ - v_{ij}\right)^2} \quad (36)$$

$$S^- = \sqrt{\sum_{i=1}^{m}\left(v^- - v_{ij}\right)^2} \quad (37)$$

$$C_j = \frac{S^-}{S^- + S^+}; 0 \le C_j \quad (38)$$

3. Results

In Section 3.1, the final GIS maps for optimal site selection have been provided. The Makran region has been divided into three areas, with the average solar and wind potential of their ideal sites imported into the HOMER software for techno-economic optimization. Section 3.2 presents the final optimization results based on the energy cost objective and estimates the decision-making variables in each feasible power supply scenario. Section 3.3 provides technical details on the renewable performance for power supply in the Makran region. Section 4.3 reveals the results of the multi-criteria decision-making process. Section 4.4 provides a comprehensive sensitivity analysis on the optimization objective, considering possible changes in input data. Finally, Section 4.5 provides more information regarding the legal requirements and facilitating regulations for the construction of renewable power plants.

3.1. GIS assessment output maps

Figure 10 illustrates the optimal sites for installing wind and solar plants in the Makran region. The heavily colored areas indicate high desirability for the construction of renewable energy power plants, while the lightly colored points represent low desirability. Based on this, specific areas in Sirik in Hormozgan province, particular points in Jask, and certain regions of Konarak, Zarabad, and Nikshahr in Sistan and Baluchestan province also have the potential for installing wind power plants.

It is worth mentioning that the majority of these regions are situated along the Makran coastal line. This location allows them to optimally harness the potential wind flow due to the absence of high elevations at sea level. Excluding the southern region of Sirik, Konarak, and Zarabad, which, despite having suitable wind potential, also experience moderate to good solar radiation. The areas in Jask and significant parts of Chabahar simultaneously benefit from high potential for installing both wind and solar power plants. Additionally, numerous coastal areas in Sistan and Baluchestan province also have the potential for utilizing photovoltaic panels. The distribution of suitable locations on the map highlights the potential for wind power plant development in the Makran region, particularly in low-population areas with vast, unused land. The results showed that more than 11% and 15% of the Makran surface are desirable or most desirable for wind and solar plant installation, respectively.

To account for the variation in renewable potential in these optimal sites in the techno-economic analysis, the Makran is divided into three areas, as indicated in Table 4. The average wind and solar radiation in the optimal sites are presented in this table and have also been imported into the HOMER software to size the power components for supplying the targeted demand.

Table 4. The average wind and solar potential in desirable and most desirable sites of the Makran

Region	Location in Makran	Main cities in the region	Average wind	Average solar radiation
R1	Western areas	Sirik and Jask	5.1-6 m/s	> 6 kWh/m^2
R2	Middle areas	Zarabad and Konarak	< 5.1 m/s	5.6-6 kWh/m^2
R3	Eastern areas	Chahbahar and Beris	> 6 m/s	< 5.6 kWh/m^2

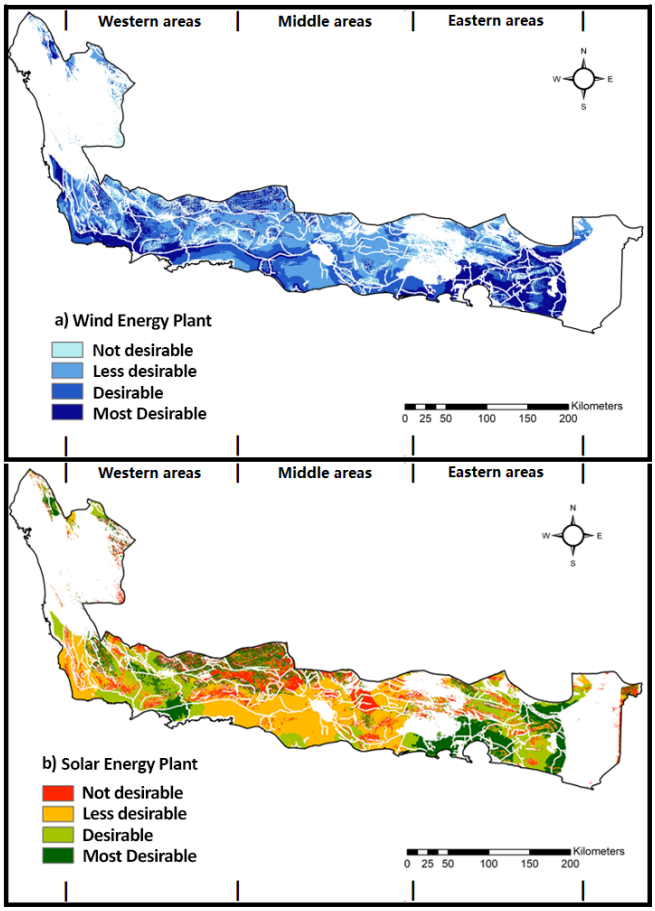

Fig. 10. GIS output maps: a) Potential sites for wind turbine plant and b) potential sites for solar plant

3.2. HOMER optimization output

Tables 5 and 6 show the variation in optimum sizing and decision-making criteria for providing high power supply reliability for the targeted demand in the Makran. Based on the results, the installation of approximately 15.4 MW of PV panels and around 3.3 MW of wind turbines has reduced the electricity purchase requirement from the grid by over 44% in the R1 area. It is noteworthy that a budget equivalent to 18.6 million dollars is required to establish such a volume of renewable resources. However, considering the 20-year operational lifespan of the project for supplying electricity to the region, the energy cost will decrease from $0.048/kWh (national grid without subsidies) to $0.042/kWh. Moreover, due to the utilizing of surplus power for desalination purposes, the energy loss from renewable sources has been reduced to less than 5%. This scenario prohibits of more than 21,000 ton/year CO_2 emissions and provide more than 99.7% power supply reliability (1-UL) for the study region. If wind turbines are not used, there will be a need to install 17.6 megawatts of solar panels. Although the energy cost will remain relatively constant, the contribution of renewable sources will decrease by 5.5% compared to the hybrid PV/WT scenario.

The addition of a WEC device (third scenario) to the power supply process in region 1 will increase the energy cost to $0.047/kWh. On the other hand, it will also improve the renewable fraction to approximately 46.5%. By removing solar panels from the optimal scenario (fourth scenario), the energy cost will increase to over $0.050/kWh. In other words, economic efficiency compared to the national grid will be compromised. Furthermore, by eliminating the

national grid, the energy cost will exceed $0.080/kWh with more than 25% excess electricity. Additionally, the cost of constructing a large stand-alone renewable power plant to achieve over 99% reliability in power supply for region 1 will exceed $100 million. Therefore, the utilization of the national grid potential in the Makran region plays a key role in achieving the economic and energy efficiency goals of the energy system.

In region 2, due to higher solar irradiance and lower wind speed, wind turbines are not included in the most economical scenario. Consequently, by installing 17.7 megawatts of solar panels, the amount of electricity purchased from the national grid can be reduced by approximately 27,000 MWh/year, resulting from a 36.3% contribution of solar energy in the power generation process. The energy cost will be around $0.044/kWh, and the initial investment requirement will be equivalent to $16.5 million. It should be noted that in region 2, the energy efficiency is higher than 95% (with less than 5% excess). Additionally, the probability of unmet electricity demand is less than 0.5% (with more than 99.5% energy security), indicating the high reliability of the energy system provided for the Makran region. If there is a need to reduce the installed capacity of solar panels, for instance, due to constraints on the installation space for these panels, it is possible to install approximately 15.9 MW PV by adding around 1.32 megawatts of wind turbines and a battery bank of about 0.6 MWh. According to the third scenario, the use of WECs in region 2 is feasible if there is limited access to large-scale wind turbines and battery banks. Additionally, WECs can be considered if there is a need to reduce the installed capacity of other renewable sources.

In region 3, due to the simultaneous desirability of wind and solar potential, the estimated capacity for installing solar panels and wind turbines is 11.9 MW and 7.3 MW, respectively. These capacities show a relatively small difference compared to the other two regions. This desirability results in a RF of over 49%, leading to an initial capital requirement of around $20 million. Despite this high initial investment, the energy cost will ultimately be less than $0.042/kWh due to the high energy production potential. It is worth noting that under these conditions, each of the wind and solar sources will generate more than 20,000 MWh/year of electricity, resulting in a reduction of approximately 25,000 tons of annual CO_2 emissions. Although this system has less than a 0.3% annual probability of power outages, the high participation of renewable sources resulted in about 6% surplus electricity. This surplus can be reduced to under 5% by increasing the daily desalination capacity. Unlike the previous regions, in region 3, by removing solar panels and installing 18 wind turbines, it is possible to achieve an energy cost of less than $0.45/kWh and a renewable fraction of over 40% (second scenario). By adding a WEC device, it is possible to reduce the installed capacity of PV panels by approximately 500 kW, and the renewable fraction will increase to over 50% (third scenario).

Therefore, it can be concluded that the use of wind turbines alongside solar panels in regions 1 and 3 provides economic efficiency and desirable energy security. However, in general, relying solely on the ideal solar potential of Makran can also achieve energy security of over 99% in all three regions. When compared to the current situation (base case), which resulted in $0.048/kWh LCOE, approximately 49,110 annual CO_2 emissions, and less than 98.5% power supply reliability, the implementation of HRESs can be advantageous for the government. Although the development of a national power grid incurs significantly lower initial costs compared to establishing renewable power plants, the long-term benefits of renewable energy are considerable. These benefits include economic, environmental, and energy security advantages. Indeed, different configurations will lead to different optimality from economic, technical, security, or environmental points of view. Therefore, it is essential to implement a multi-criteria decision-making process based on the HOMER results.

Table 5. Optimal sizing of feasible power supply scenarios

Code	HRES Configuration	PV (MW)	WT (units)	WEC (unit)	Batter (MWh)	Conv (MW)	Grid (MWh)
R1-1	Grid/PV/WT	15.4	5	–	–	10.9	41554.7
R1-2	Grid/PV	17.6	–	–	–	12.1	45608.3
R1-3	Grid/PV/WT/WEC	14.9	5	1	–	10.5	40146.9
R1-4	Grid/WT/WEC	–	16	1	–	–	49079.7
R1-5	PV/WT/WEC/Battery	48.6	9	1	151.6	24.7	-
R2-1	Grid/PV	17.7	–	–	–	11.7	47675.2
R2-2	Grid/PV/WT/Battery	15.9	2	–	0.662	11.1	47274.5
R2-3	Grid/PV/WT/WEC	16.7	1	1	–	11.4	45430.5
R2-4	Grid/WT/WEC	–	10	1	–	–	60054.5
R2-5	PV/WT/WEC/Battery	67.8	12	1	153.9	26.6	-
R3-1	Grid/PV/WT	11.9	11	–	–	8.2	38243.2
R3-2	Grid/WT	–	18	–	–	–	44051.3
R3-3	Grid/PV/WT/WEC	11.4	11	1	–	7.7	36891.6
R3-4	Grid/PV/WEC	11.4	–	1	–	11.4	46918.5
R3-5	PV/WT/Battery	47.1	25	–	147.3	26.1	-
R0	Grid	-	-	-	-	-	74334.9

Table 6. The output values of decision-making objectives in each feasible power supply scenario

Code	COE ($/kWh)	IC (M$)	RF (%)	CO_2 (ton/yr)	EXL (%)	UL (%)	Resources Diversity
R1-1	0.042	18.6	44.6	27.5	4.73	0.28	3
R1-2	0.043	16.6	39.1	30.1	4.81	0.35	2
R1-3	0.047	22.8	46.5	26.5	4.65	0.27	4
R1-4	0.052	17.6	34.4	32.4	3.95	0.56	3
R1-5	0.085	100.9	100	0	28.1	0.73	3
R2-1	0.044	16.5	36.3	31.4	4.41	0.46	2
R2-2	0.045	16.7	36.8	31.2	3.17	0.45	3
R2-3	0.049	21.3	39.3	30.0	4.10	0.43	4
R2-4	0.055	12.8	19.4	39.71	0.71	0.85	3
R2-5	0.099	119.9	100	0	42.8	1.04	3
R3-1	0.042	20.0	49.1	25.3	6.32	0.29	3
R3-2	0.044	14.5	41.2	29.1	6.84	0.44	2
R3-3	0.046	24.3	50.8	24.4	6.55	0.28	4
R3-4	0.049	21.0	37.3	30.9	3.71	0.47	3
R3-5	0.090	106.9	100	0	39.9	0.91	2
R0	0.048	0	0	49.2	0	1.5	1

3.3. Techno-economic analysis

The levelized cost of power generation (LCOE) for each component can be defined as the ratio of the component cost to its total power during the project lifetime. The results showed that the LCOE for PV varies between 0.02 to 0.03 $/kWh, and for WT, it ranges between 0.03 to 0.05 $/kWh. Furthermore, it is about 0.18 $/kWh in

distances lower than 50 km from the coastline for the WEC technology. The main reason for this high cost is the high capital and O&M cost of WECs and also the low wave heights in the Oman Sea near the Makran coast. Therefore, the PV and WT technologies are the most affordable renewable options for Makran, where the PV shows almost constant LCOE while WT shows lower LCOEs at the eastern regions due to higher wind potential. Fig. 11 displays the annual power output profile of components for a typical reliable power supply scenario in Region 3, identified as the most economic area to apply hybrid renewable resources.

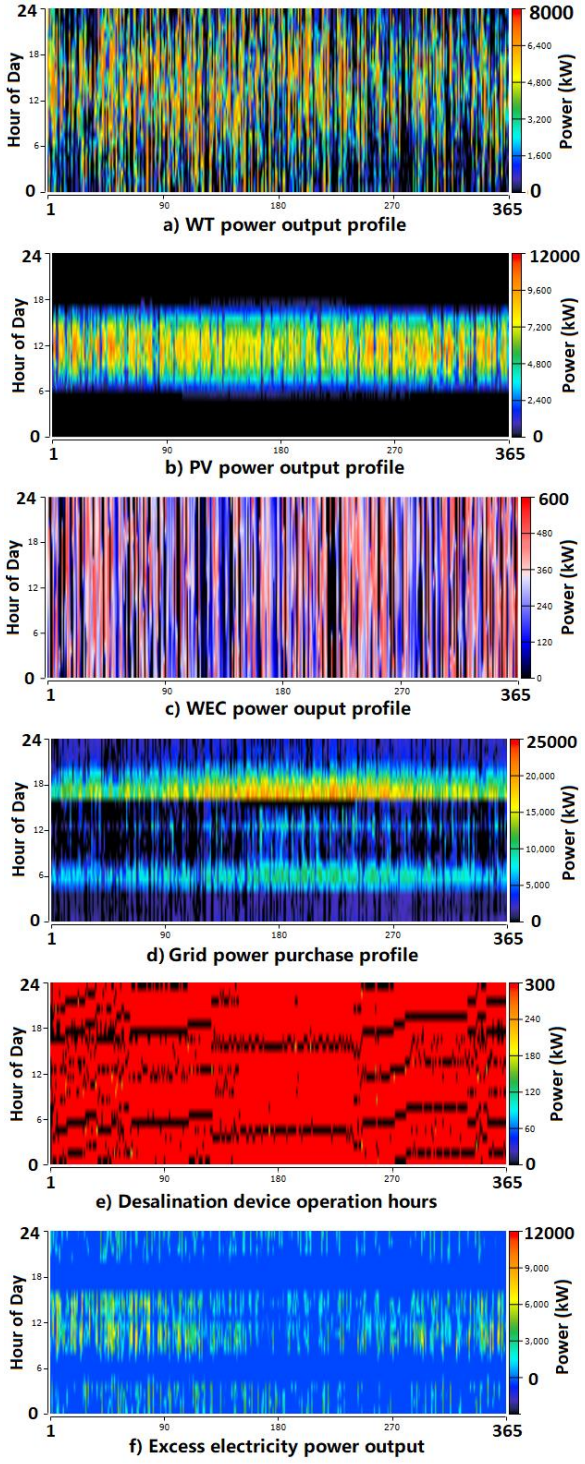

Fig. 11. Power output profiles of components in the Makran area

Accordingly, solar power generation is suitable throughout the year. According to part (d) of this figure, power purchases from the grid significantly decrease during PV power production hours, even during peak power consumption hours. Furthermore, wind power generation can effectively complement the solar power profile due to its ability to generate power during the night hours. However, based on the wind turbine power profile, the power generation potential of wind turbines in the first half of the year is higher than in the second half. Furthermore, as indicated in part (c) of this figure, the WEC is capable of providing power throughout the year. However, it's important to note that the timesteps with near-rated power output are limited, and the cut-off condition can occur for longer periods compared to wind turbine technology. Therefore, considering the lower economic viability of WEC compared to WT and the superior technical performance of WT over WEC, wind turbine technology emerges as the more suitable option to be combined with solar energy in the Makran region.

According to part (e) of Fig. 11, the desalination device is effectively supplied by the combination of the grid and excess renewable power. The desalination plant pumps are activated near peak hours or when the renewable output potential significantly reduces. This approach, as indicated in part (f) of this figure, eliminates the high levels of renewable excess power and results in a final excess electricity of less than 4 GWh/year (or approximately 5%).

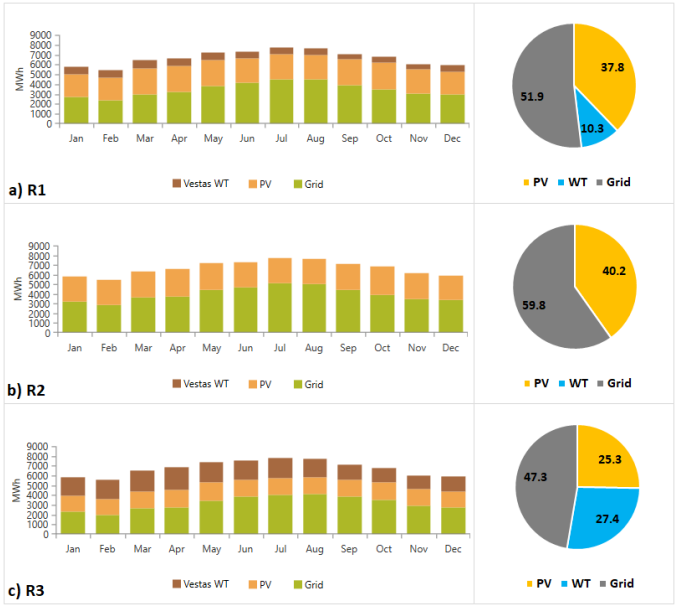

Fig. 12. Comparison of participation of renewable energies in final power supply in each region.

Fig. 12 illustrates the monthly and annual participation of each technology in the most economic power supply scenario in different regions of Makran. Accordingly, more than 48% of power generation has been contributed by renewables in R3 and R1, while in R2, this value decreases to about 40%. Furthermore, this contribution is more significant in months with moderate and not-warm ambient temperatures, due to lower demand and the lesser impact of temperature on the output of PV plants. This figure illustrates that renewables can effectively participate in reducing dependency on the grid and enhancing energy security throughout all months of the year.

3.4. Multi-criteria decision-making outputs

The results of the MCDM analysis (Fig. 13) indicate that regions 1 and 3 exhibit a higher potential for the integration of renewable resources. For the coastal cities of Chabahar and Beris in study area

R3, the use of a combined renewable energy system (Grid/PV/WT) with an energy cost of $0.042/kWh and a 49% RF has been identified. The scenario with the Grid/PV/WT/WEC configuration also shows a nearly similar TOPSIS coefficient. In study area R1, particularly in coastal cities such as Jask and Sirik, the Grid/PV/WT/WEC system with a COE of $0.047/kWh and a 46% RF demonstrates a higher coefficient compared to other scenarios. Additionally, the Grid/PV/WT system has been optimized in this scenario, indicating a similar performance of renewable sources in ensuring energy security in the first and third study areas.

In study area 2, especially in coastal cities like Konarak and Zarabad, the Grid/PV/WT/Battery and Grid/PV/WT/WEC scenarios with a COE below $0.049/kWh and an approximately 36% RF have been identified as efficient scenarios. In region 2, where the renewable potential is slightly lower, the use of a battery bank has been incorporated into the optimal scenario. Moreover, for all scenarios, the utilization of wave energy has proven to be superior among alternative options. Despite the increased energy cost, it has been employed to diversify the energy production sources and enhance energy security. It should be noted that the current energy situation of Makran (R0) with a TOPSIS coefficient of less than 0.6 shows much lower optimality compared to the renewable-based energy systems.

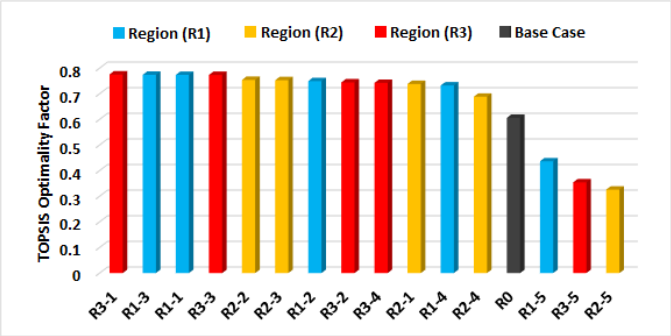

Fig. 13. Multi-criteria decision-making optimality factor for different HRES configurations

3.5 Sensitivity Analysis

Figures 14 and 15 show the sensitivity of energy cost and environmental performance in the optimal scenario, based on possible changes in the capital costs of renewable-based technologies and local renewable resource potential. To this end, capital cost variations ranging from $400 to $1,200 per kW for PV panels, $600 to $1,800 per kW for wind turbines, and a 50% potential change for capital cost of other critical components and renewable resources potential have been considered.

Accordingly, even with a more than 30% increase in the price of solar panels and a 50% increase in the price of wind turbines compared to initial costs (part a), the cost of energy to ensure energy security (covering potential blackouts) in the region can remain below $0.05/kWh. However, due to the reduced economic viability of renewable resources, carbon dioxide emissions, compared to current conditions, are projected to increase from 27,000 tons to 31,000 tons per year (equivalent to a 15% rise). As shown, changes in WEC technology prices and battery bank costs have no significant effect on COE variations (parts b and c), as these two components are absent in most optimal scenarios. Therefore, their price variations do not influence the optimal COE. Although a 50% change in the cost of the converter component can lead to COE variations between $0.041 and $0.043 per kWh, this difference is negligible compared to the $0.042/kWh in the optimal scenario determined by the MCDM process.

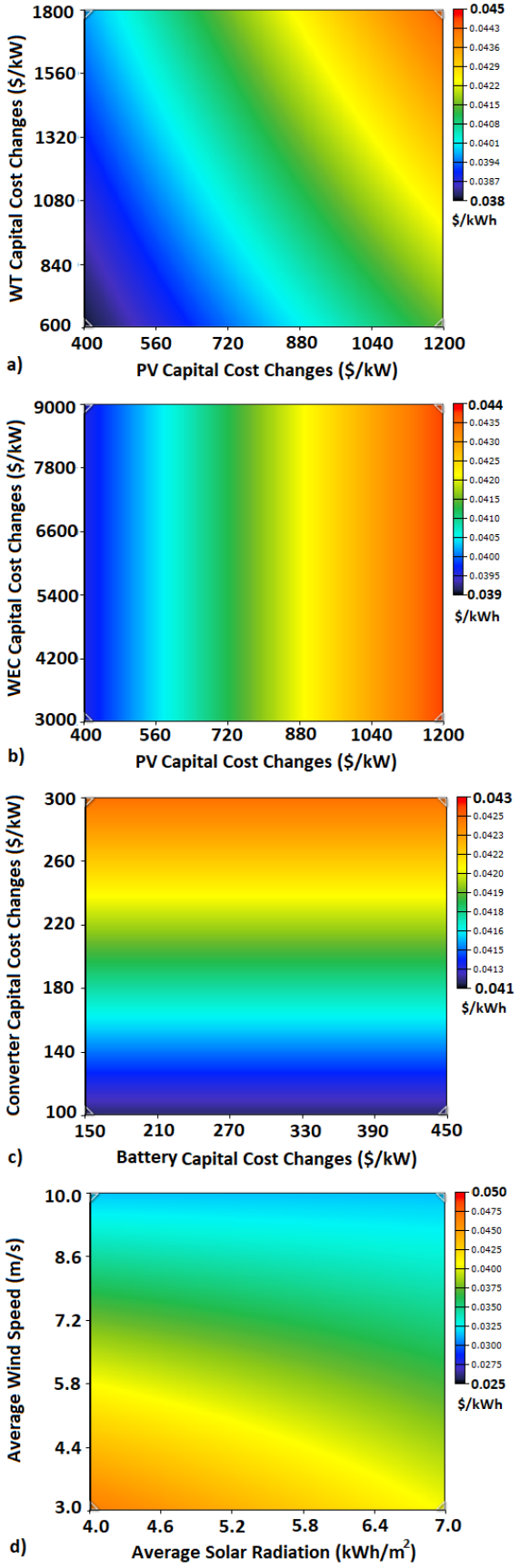

Fig. 14. Economic sensitivity analysis based on potential changes in component capital costs and renewable resource availability

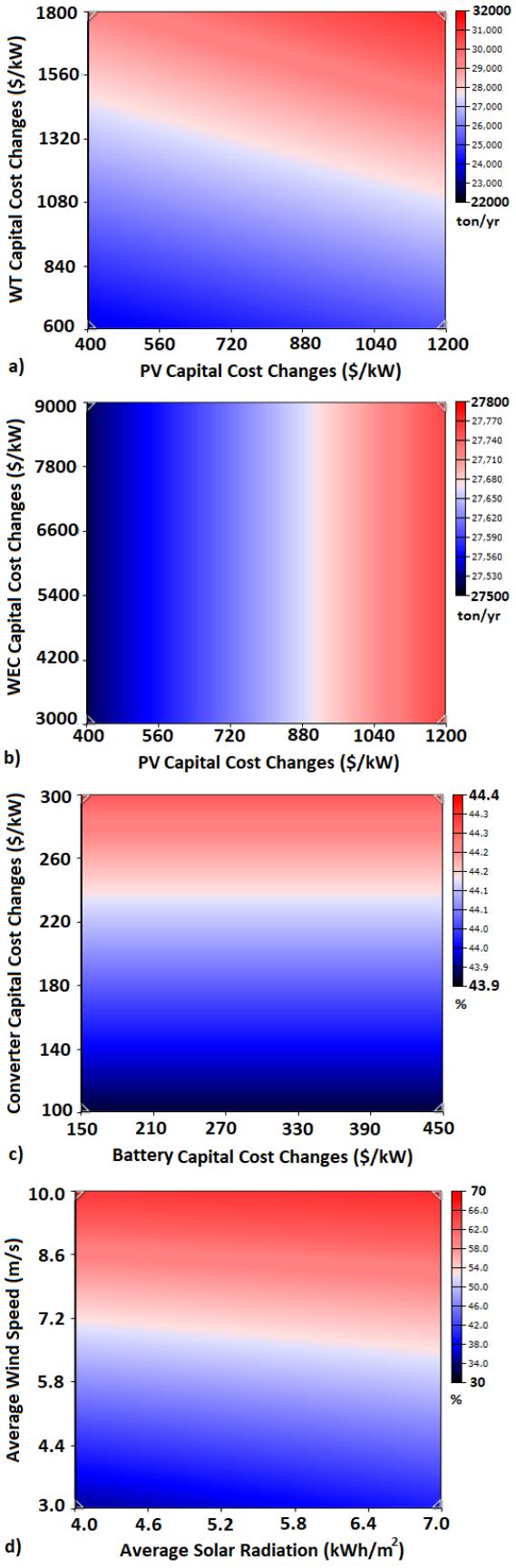

Fig. 15. Environmental sensitivity analysis based on potential changes in capital costs and renewable resource availability

Changes in renewable resource potential (part d) have a significant effect on the renewable fraction and energy cost. However, in the identified optimal locations with above-average renewable resource potential, the COE will be less than $0.045, and the renewable fraction will exceed 40%, which is acceptable for high renewable penetration energy systems. The sensitivity analysis of the optimal scenario indicates that an increase in the price of renewable components can be compensated for by an increased contribution from the grid, albeit at the cost of higher final emissions. In the Makran region, under both the least and most favorable renewable potentials, renewable resources combined with the national grid can ensure energy security at a COE ranging from $0.035 to $0.050 per kWh. However, if renewable resources are deployed in non-optimal locations, the share of renewable energy will drop to less than 35%, leading to approximately 65% reliance on the national grid. Therefore, the optimal HRES scenario demonstrates strong resilience against potential changes in renewable resource availability and capital costs, particularly when optimal locations for renewable plant installations are identified.

3.6 Discussion on legal requirements and regulations

This section provides a summary of the potential benefits of the latest regulations from Iran's Energy Council for developing an optimized renewable energy system. The optimum renewable energy system in this study demonstrated a renewable contribution of over 30% to the final power supply and, on average, reduced fossil fuel-based grid dependency by 40% (equivalent to natural gas saving in power supply). According to Tehran Chamber of Commerce report [51], three main regulations in Iran can now support the development of such a system:

- The guaranteed purchase of electricity through Article-61 of the Energy Consumption Reform Act: Accordingly, investors who intend to establish renewable power plants with a capacity of less than one megawatt can sell their generated electricity to the government at a fixed rate for a period of 20 years. This law can help distribute the optimized renewable capacity outlined in this study among various private sector suppliers.
- Utilization of Article-12 of the Law for Removing Barriers to Competitive Production: According to this plan, the government is obligated to compensate investors whose goods or services lead to fuel savings by reimbursing an amount equivalent to the saved fuel, up to the principal and interest of the investment. Therefore, investors who win tenders for establishing renewable power plants organized by SATBA can benefit from this fixed income for a minimum of six years in the under-study area.
- Commitment of Government Agencies, Public Entities, and Industrial Units: in accordance with Article-50 of Iran's Sixth and seventh Development Plan, the government is obligated to ensure that at 5% of the country's power generation capacity comes from renewable and clean energy sources. Accordingly, public entities are required to supply 20% of their electricity consumption from renewable energy sources within four years; otherwise, they will face fines at renewable energy rates. Additionally, in line with Article-16 of the Law for the Development of Knowledge-Based Production, industrial units with a consumption capacity of more than one megawatt are obligated to source 1% of their electricity annually, increasing to at least 5% by the fifth year, through the establishment of renewable power plants. Therefore, public and commercial units in the region can participate in attracting investment to install the necessary renewable energy capacity.

It is important to note that, although the most significant legal limitation for establishing renewable power plants is related to environmental concerns, this study conducted an optimal location assessment based on these restrictions. The results demonstrated that the Makran region holds significant potential for harnessing renewable energy sources.

4. Conclusions

In this study, the feasibility of implementing renewable-based hybrid energy systems along the southern coasts of Iran has been analyzed through geographical feasibility studies and techno-economic optimization. The Makran area, situated near the Oman Sea, was chosen as a case study to fulfill the energy demands of 50,000 residents. The results indicate that:

- Approximately 11% and 15% of the Makran area are deemed suitable for wind turbine and photovoltaic plant installations, respectively. The cities of Jask, Chahbahar, Konarak, and Beris exhibited the highest ideal surfaces based on climatic, topological, environmental, and technically available conditions. All regions in Makran displayed solar radiation levels exceeding 5.4 kWh/m². Additionally, the GIS assessment identified areas with an average wind speed of more than 6 m/s, making the application of hybrid PV/WT systems particularly ideal for improving local grid reliability.
- The hybrid PV/WT/Grid system, with an energy cost of less than $0.045/kWh and a renewable fraction exceeding 30%, has been identified as the optimal solution for enhancing the energy security of the local grid. This involves diversifying power supply resources and achieving a reduction in grid dependency ranging between 30% to 50%. The findings indicate that the government can achieve this goal by installing approximately 19 MW of renewables, primarily from solar power plants, with an initial cost of less than $25 million.
- The results of the MCDM process revealed that both PV/WT/Grid and PV/WT/WEC/Grid configurations have similar optimality factors. They achieve over 99.7% power supply reliability and affordable energy costs by utilizing 30-50% renewable resources compared to non-subsidized energy tariffs. Although the integration of wave energy converters resulted in higher LCOEs, they demonstrated optimality in reducing the required capacity of other renewable components in cases such as limited land availability for installation and technological constraints.
- The utilization of excess power from renewables in reverse osmosis (RO) plants reduces the final excess electricity production from over 15% to less than 5%, indicating that this approach is a suitable option for areas near the sea facing water scarcity. Although the return on investment for large-scale renewable power plant installations in Iran is limited to approximately 12 years, the results demonstrate several positive side effects. These include a reduction in LPSP from 1.5% to 0.3%, a decrease of approximately 25,000 tons in annual CO_2 emissions, and reduced dependency on fossil fuels. These factors make grid-connected HRESs particularly attractive for the southern coasts of Iran.

For future studies, it is suggested to analyze the effect of implementing bio-based renewable power generation in coastal areas, in conjunction with the analysis of renewable resources, to enhance power supply flexibility. Additionally, conducting a feasibility study on utilizing the remaining excess electricity for hydrogen production could be an attractive avenue for large-scale renewable power plants. Generating electricity from this hydrogen or injecting it into local gas pipelines can help with peak shaving or reducing fossil fuel dependency in stand-alone energy systems.

Appendix A. Techno-economic input data of the HRES

Power Component	**Specifications**
Wind Turbine [12]	**Data**
Type in HOMER	Vestas V47
Local service provider	MAPNA Co.
Rated power per device	660 kW
Rotor diameter	47 m
Hub height	40 m
Cut in – cut off wind speed	4-25 m/s
Lifetime	20 years
Capital cost	$1200/kW
Capital cost sensitivity analysis range	600-1800 $/kW
Maintenance cost	3% capital
PV Module [52]	**Data**
Type in HOMER	LONGI LR360
Local service provider	Noursun Co.
Rated power per module	350 W
Operating Temperature (NOCT)	45°C
Temperature coefficient of power	0.41%/°C
Efficiency	18.1%
Lifetime	20 years
Capital cost	$800/kW
Capital cost sensitivity analysis range	400-1200 $/kW
Maintenance cost	1% capital
Wave energy converter (WEC) [12]	**Data**
Imported device to the HOMER	PELAMIS 750
International service provider	PELAMIS Co.
Rated power per device	750 kW
Cut in – cut off wave height	1-12 m
Approximate body length	250 m
Lifetime	20 years
Capital cost	$6000/kW
Capital cost sensitivity analysis range	3000-9000 $/kW
Maintenance cost	3% capital
Battery unit [25]	**Data**
Storage Type	Li-ion bank
Rated power per module	100 kWh
International service provider	Jingsun Co.
Roundtrip Efficiency	90%
Lifetime	15 years
Nominal Capacity	167 Ah
Throughput	300000 kWh
Capital cost	$300/kWh
Capital cost sensitivity analysis range	150-450 $/kW
Maintenance cost	1% capital
Power Converter [53]	**Data**
Local service provider	Noursun Co.
Inverter Efficiency	95%
Rectifier Efficiency	90%
Lifetime	10 years
Capital cost	$200/kW
Capital cost sensitivity analysis range	100-300 $/kW
Maintenance cost	1% capital
Power Grid [48]	**Data**
Max annual capacity shortage	2%
Peak-shoulder-off peak tariffs	0.03-0.05-0.06 $/kWh
CO_2 Emission factor	660.6 g/kWh
Main possible outage times	Summer afternoon hours
Project	**Data**
Project life time	20 years
Inflation rate	25%
Discount rate	23%
Maximum LPSP	2%

References

[1] Nasouri M, Delgarm N. Bushehr Nuclear Power Plants (BNPPs) and the perspective of sustainable energy development in Iran. Prog Nucl Energy 2022;147:104179. https://doi.org/10.1016/j.pnucene.2022.104179.

[2] Sadovskaia K, Bogdanov D, Honkapuro S, Breyer C. Power transmission and distribution losses – A model based on available empirical data and future trends for all countries globally. Int J Electr Power Energy Syst 2019;107:89–109. https://doi.org/10.1016/j.ijepes.2018.11.012.

[3] NATO. Energy Management in a Military Expeditionary Environment: an assessment of three energy management case studies in operational settings. 2019.

[4] Tamjid Shabestari S, Kasaeian A, Vaziri Rad MA, Forootan Fard H, Yan W-M, Pourfayaz F. Techno-financial evaluation of a hybrid renewable solution for supplying the predicted power outages by machine learning methods in rural areas. Renew Energy 2022;194:1303–25. https://doi.org/10.1016/j.renene.2022.05.160.

[5] SATBA. Renewable energy statics of Iran. Organ Renew Energy Electr Energy Effic Iran 2023. https://www.satba.gov.ir/en/home (accessed October 10, 2023).

[6] REN21. Renewables in Energy Supply. Renewables Now 2023.

[7] Ghasemi G, Noorollahi Y, Alavi H, Marzband M, Shahbazi M. Theoretical and technical potential evaluation of solar power generation in Iran. Renew Energy 2019;138:1250–61. https://doi.org/https://doi.org/10.1016/j.renene.2019.02.068.

[8] Razeghi M, Hajinezhad A, Naseri A, Noorollahi Y, Moosavian SF. Multi-criteria decision-making for selecting a solar farm location to supply energy to reverse osmosis devices and produce freshwater using GIS in Iran. Sol Energy 2023;253:501–14. https://doi.org/https://doi.org/10.1016/j.solener.2023.01.029.

[9] Hooshangi N, Gharakhanlou NM, Ghaffari Razin SR. Evaluation of potential sites in Iran to localize solar farms using a GIS-based Fermatean Fuzzy TOPSIS. J Clean Prod 2023;384:135481. https://doi.org/https://doi.org/10.1016/j.jclepro.2022.135481.

[10] Asadi M, Pourhossein K, Mohammadi-Ivatloo B. GIS-assisted modeling of wind farm site selection based on support vector regression. J Clean Prod 2023;390:135993. https://doi.org/https://doi.org/10.1016/j.jclepro.2023.135993.

[11] Razavi Dehkordi MH, Meghdadi Isfahani AH, Rasti E, Nosouhi R, Akbari M, Jahangiri M. Energy-Economic-Environmental assessment of solar-wind-biomass systems for finding the best areas in Iran: A case study using GIS maps. Sustain Energy Technol Assessments 2022;53:102652. https://doi.org/https://doi.org/10.1016/j.seta.2022.102652.

[12] Jahangir MH, Shahsavari A, Vaziri Rad MA. Feasibility study of a zero emission PV/Wind turbine/Wave energy converter hybrid system for stand-alone power supply: A case study. J Clean Prod 2020;162:2075–95. https://doi.org/10.1016/j.jclepro.2020.121250.

[13] Jahangir MH, Mazinani M. Evaluation of the convertible offshore wave energy capacity of the southern strip of the Caspian Sea. Renew Energy 2020. https://doi.org/10.1016/j.renene.2020.01.012.

[14] Kamranzad B, Chegini V. Study of Wave Energy Resources in Persian Gulf : Seasonal and Monthly Distributions. 11th Int Conf Coasts, Ports Mar Struct (ICOPMAS 2014) 2014:658–61. https://doi.org/10.13140/RG.2.1.2990.2249.

[15] Rashid A, Hasanzadeh S. Status and potentials of offshore wave energy resources in Chahbahar area (NW Omman Sea). Renew Sustain Energy Rev 2011;15:4876–83. https://doi.org/10.1016/j.rser.2011.06.015.

[16] Cyprien Bosserelle, Sandeep Reddy JK. Cost Analysis of Wave Energy in the Pacific. 2015.

[17] Nasrollahi S, Kazemi A, Jahangir M-H, Aryaee S. Selecting suitable wave energy technology for sustainable development, an MCDM approach. Renew Energy 2022;202:756–72. https://doi.org/10.1016/j.renene.2022.11.005.

[18] Asrari A, Ghasemi A, Javidi MH. Economic evaluation of hybrid renewable energy systems for rural electrification in Iran - A case study. Renew Sustain Energy Rev 2012. https://doi.org/10.1016/j.rser.2012.02.052.

[19] Baneshi M, Hadianfard F. Techno-economic feasibility of hybrid diesel/PV/wind/battery electricity generation systems for non-residential large electricity consumers under southern Iran climate conditions. Energy Convers Manag 2016;127:233–44. https://doi.org/10.1016/j.enconman.2016.09.008.

[20] Jahangiri M, Yousefi Y, Pishkar I, Jalaladdin S, Dehshiri H. Techno–Econo–Enviro Energy Analysis, Ranking and Optimization of Various Building-Integrated Photovoltaic (BIPV) Types in Different Climatic Regions of Iran. Energies 2023;16(1):546.

[21] Kasaeian A, Rahdan P, Rad MAV, Yan W-M. Optimal design and technical analysis of a grid-connected hybrid photovoltaic/diesel/biogas under different economic conditions: A case study. Energy Convers Manag 2019;198:111810. https://doi.org/10.1016/j.enconman.2019.111810.

[22] Jahangir MH, Fakouriyan S, Amin M, Rad V. Feasibility study of on / off grid large-scale PV / WT / WEC hybrid energy system in coastal cities : A case-based research. Renew Energy 2020;162:2075–95. https://doi.org/10.1016/j.renene.2020.09.131.

[23] Katsivelakis M, Bargiotas D, Daskalopulu A, Panapakidis IP, Tsoukalas L. Techno-economic analysis of a stand-alone hybrid system: Application in donoussa island, greece. Energies 2021;14:1–31. https://doi.org/10.3390/en14071868.

[24] Azaroual M, Ouassaid M, Maaroufi M. Model predictive control-based energy management strategy for grid-connected residential photovoltaic–wind–battery system. INC; 2021. https://doi.org/10.1016/b978-0-12-820004-9.00014-0.

[25] Amin M, Rad V, Kasaeian A, Niu X, Zhang K, Mahian O. Excess electricity problem in off-grid hybrid renewable energy systems : A comprehensive review from challenges to prevalent solutions. Renew Energy 2023;212:538–60. https://doi.org/10.1016/j.renene.2023.05.073.

[26] Islam S, Akhter R, Ashifur M. A thorough investigation on hybrid application of biomass gasi fi er and PV resources to meet energy needs for a northern rural off-grid region of Bangladesh : A potential solution to replicate in rural off-grid areas or not ? Energy 2018;145:338–55. https://doi.org/10.1016/j.energy.2017.12.125.

[27] Alsagri AS, Alrobaian AA, Nejlaoui M. Techno-economic evaluation of an off-grid health clinic considering the current and future energy challenges: A rural case study. Renew Energy 2021;169:34–52. https://doi.org/10.1016/j.renene.2021.01.017.

[28] Das P, Das BK, Rahman M, Hassan R. Evaluating the prospect of utilizing excess energy and creating employments from a hybrid energy system meeting electricity and freshwater demands using multi-objective evolutionary algorithms. Energy 2022;238. https://doi.org/10.1016/j.energy.2021.121860.

[29] Amin M, Rad V, Shahsavari A, Rajaee F, Kasaeian A. Techno-economic assessment of a hybrid system for energy supply in the affected areas by natural disasters : A case study. Energy Convers Manag 2020;221:113170. https://doi.org/10.1016/j.enconman.2020.113170.

[30] Shahsavari A, Vaziri Rad MA, Pourfayaz F, Kasaeian A. Optimal sizing of an integrated CHP and desalination system as a polygeneration plant for supplying rural demands. Energy

2022;258:124820. https://doi.org/10.1016/j.energy.2022.124820.

[31] Al-Karaghouli A, Kazmerski LL. Energy consumption and water production cost of conventional and renewable-energy-powered desalination processes. Renew Sustain Energy Rev 2013;24:343–56. https://doi.org/10.1016/j.rser.2012.12.064.

[32] Padrón I, Avila D, Marichal GN, Rodríguez JA. Assessment of Hybrid Renewable Energy Systems to supplied energy to Autonomous Desalination Systems in two islands of the Canary Archipelago. Renew Sustain Energy Rev 2019;101:221–30. https://doi.org/10.1016/j.rser.2018.11.009.

[33] PMO. Download of Oman Sea and Persian Gulf Wave Characteristics. Ports Marit Organ Iran 2022. https://www.pmo.ir/ (accessed January 1, 2022).

[34] NASA. NASA Data Access viewer. Meteorol Data 2023. https://power.larc.nasa.gov/data-access-viewer/ (accessed January 1, 2024).

[35] Saaty T. The Analytical Hierarchy process, planning, priority, Resource Allocation. McGraw-Hill Int B Co 1980.

[36] Dehghan H, Pourfayaz F, Shahsavari A. Multicriteria decision and Geographic Information System-based locational analysis and techno-economic assessment of a hybrid energy system. Renew Energy 2022;198:189–99. https://doi.org/10.1016/j.renene.2022.07.147.

[37] Ali S, Taweekun J, Techato K, Waewsak J, Gyawali S. GIS based site suitability assessment for wind and solar farms in Songkhla, Thailand. Renew Energy 2019;132:1360–72. https://doi.org/10.1016/j.renene.2018.09.035.

[38] Al-Yahyai S, Charabi Y, Gastli A, Al-Badi A. Wind farm land suitability indexing using multi-criteria analysis. Renew Energy 2012;44:80–7. https://doi.org/10.1016/j.renene.2012.01.004.

[39] Messaoudi D, Settou N, Negrou B, Rahmouni S, Settou B, Mayou I. Site selection methodology for the wind-powered hydrogen refueling station based on AHP-GIS in Adrar, Algeria. Energy Procedia, 2019, p. 67–76. https://doi.org/10.1016/j.egypro.2019.04.008.

[40] Noorollahi Y, Yousefi H, Mohammadi M. Multi-criteria decision support system for wind farm site selection using GIS. Sustain Energy Technol Assessments 2016;13:38–50. https://doi.org/10.1016/j.seta.2015.11.007.

[41] Xu Y, Li Y, Zheng L, Cui L, Li S, Li W, et al. Site selection of wind farms using GIS and multi-criteria decision making method in Wafangdian, China. Energy 2020;207:118222. https://doi.org/10.1016/j.energy.2020.118222.

[42] SolarGIS. Global Solar Atlas 2.0, a free, web-based application is developed and operated by the company Solargis s.r.o. on behalf of the World Bank Group, utilizing Solargis data, with funding provided by the Energy Sector Management Assistance Program (ESMAP). Fo. World Bank 2023.

[43] HOMER Energy. HOMER Pro 3.13 User Manual. NREL 2020. https://www.homerenergy.com/products/pro/docs/index.html (accessed January 1, 2023).

[44] Toopshekan A, Rahdan P, Vaziri Rad MA, Yousefi H, Astaraei FR. Evaluation of a stand-alone CHP-Hybrid system using a multi-criteria decision making due to the sustainable development goals. Sustain Cities Soc 2022;87:104170. https://doi.org/10.1016/j.scs.2022.104170.

[45] Toopshekan, Ashkan Abedian A, Azizi A, Ahmadi E, Vaziri Rad MA. Optimization of a CHP system using a forecasting dispatch and teaching-learning-based optimization algorithm. Energy 2023;285:128671. https://doi.org/10.1016/j.energy.2023.128671.

[46] Vaziri Rad MA, Kasaeian A, Mahian O, Toopshekan A. Technical and economic evaluation of excess electricity level management beyond the optimum storage capacity for off-grid renewable systems. J Energy Storage 2024;87:111385. https://doi.org/10.1016/j.est.2024.111385.

[47] Toopshekan A, Ahmadi E, Abedian A, Vaziri Rad MA. Techno-economic analysis, optimization, and dispatch strategy development for renewable energy systems equipped with Internet of Things technology. Energy 2024;296:131176. https://doi.org/10.1016/j.energy.2024.131176.

[48] Vaziri Rad MA, Toopshekan A, Rahdan P, Kasaeian A, Mahian O. A comprehensive study of techno-economic and environmental features of different solar tracking systems for residential photovoltaic installations. Renew Sustain Energy Rev 2020;129:109923. https://doi.org/10.1016/j.rser.2020.109923.

[49] Rad M, Kasaeian A, Mahian O. Evaluation of stand-alone hybrid renewable energy system with excess electricity minimizer predictive dispatch strategy. Energy Convers Manag 2024;299:117898. https://doi.org/10.1016/j.enconman.2023.117898.

[50] Vaziri Rad MA, Forootan Fard H, Khazanedari K, Toopshekan A, Ourang S, Khanali M, et al. A global framework for maximizing sustainable development indexes in agri-photovoltaic-based renewable systems: Integrating DEMATEL, ANP, and MCDM methods. Appl Energy 2024;360:122715. https://doi.org/https://doi.org/10.1016/j.apenergy.2024.122715.

[51] Asadi A, Vaziri Rad M. Global Trends in Renewable Energy Investment. Econ Res Dep Tehran Chamb Commer (Refer to Seas 11) 2024:1–80. https://economy.tccim.ir/fulldoc?nid=2131 (accessed September 9, 2024).

[52] Mousavi SA, Toopshekan A, Mehrpooya M, Delpisheh M. Comprehensive exergetic performance assessment and techno-financial optimization of off-grid hybrid renewable configurations with various dispatch strategies and solar tracking systems. Renew Energy 2023;210:40–63. https://doi.org/10.1016/j.renene.2023.04.018.

[53] Zamanpour K, Vaziri Rad MA, Saberi N, Fereidooni L, Kasaeian A. Techno-economic comparison of dispatch strategies for stand-alone industrial demand integrated with fossil and renewable energy resources. Energy Reports 2023;10:2962–81. https://doi.org/https://doi.org/10.1016/j.egyr.2023.09.095.